AMERICAN SOCIETY FOR MICROBIOLOGY | Journal of Virology®

VACCINES AND ANTIVIRAL AGENTS

Highly Neutralizing COVID-19 Convalescent Plasmas Potently Block SARS-CoV-2 Replication and Pneumonia in Syrian Hamsters

Yuki Takamatsu,[a] Masaki Imai,[b] Kenji Maeda,[a] Noriko Nakajima,[c] Nobuyo Higashi-Kuwata,[a] Kiyoko Iwatsuki-Horimoto,[b] Mutsumi Ito,[b] Maki Kiso,[b] Tadashi Maemura,[b] Yuichiro Takeda,[d] Kazumi Omata,[e,f] Tadaki Suzuki,[c] Yoshihiro Kawaoka,[b,g,h] Hiroaki Mitsuya[a,i,j]

[a]Department of Refractory Viral Infections, National Center for Global Health and Medicine Research Institute, Tokyo, Japan
[b]Division of Virology, Department of Microbiology and Immunology, Institute of Medical Science, University of Tokyo, Tokyo, Japan
[c]Department of Pathology, National Institute of Infectious Diseases, Tokyo, Japan
[d]Department of Respiratory Medicine, Center Hospital of the National Center for Global Health and Medicine, Tokyo, Japan
[e]Center for Clinical Sciences, National Center for Global Health and Medicine, Tokyo, Japan
[f]Departments of Hematology, Rheumatology, and Infectious Diseases, Kumamoto University Hospital, Kumamoto, Japan
[g]Influenza Research Institute, Department of Pathobiological Sciences, School of Veterinary Medicine, University of Wisconsin-Madison, Madison, Wisconsin, USA
[h]Department of Special Pathogens, International Research Center for Infectious Diseases, Institute of Medical Science, University of Tokyo, Tokyo, Japan
[i]Experimental Retrovirology Section, Center for Cancer Research, National Cancer Institute, National Institutes of Health, Bethesda, Maryland, USA
[j]Department of Clinical Sciences, Kumamoto University School of Medicine, Kumamoto, Japan

ABSTRACT Despite various attempts to treat severe acute respiratory syndrome coronavirus 2 (SARS-CoV-2)-infected patients with COVID-19 convalescent plasmas, neither appropriate approach nor clinical utility has been established. We examined the efficacy of administration of highly neutralizing COVID-19 convalescent plasma (*hn*-plasmas) and such plasma-derived IgG administration using the Syrian hamster COVID-19 model. Two *hn*-plasmas, which were in the best 1% of 340 neutralizing activity-determined convalescent plasmas, were intraperitoneally administered to SARS-CoV-2-infected hamsters, resulting in a significant reduction of viral titers in lungs by up to 32-fold compared to the viral titers in hamsters receiving control nonneutralizing plasma, while with two moderately neutralizing plasmas (*mn*-plasmas) administered, viral titer reduction was by up to 6-fold. IgG fractions purified from the two *hn*-plasmas also reduced viral titers in lungs more than those from the two *mn*-plasmas. The severity of lung lesions seen in hamsters receiving *hn*-plasmas was minimal to moderate as assessed using microcomputerized tomography, which histological examination confirmed. Western blotting revealed that all four COVID-19 convalescent plasmas variably contained antibodies against SARS-CoV-2 components, including the receptor-binding domain and S1 domain. The present data strongly suggest that administering potent neutralizing activity-confirmed COVID-19 convalescent plasmas would be efficacious in treating patients with COVID-19.

IMPORTANCE Convalescent plasmas obtained from patients who recovered from a specific infection have been used as agents to treat other patients infected with the very pathogen. To treat using convalescent plasmas, despite that more than 10 randomized controlled clinical trials have been conducted and more than 100 studies are currently ongoing, the effects of convalescent plasma against COVID-19 remained uncertain. On the other hand, certain COVID-19 vaccines have been shown to reduce the clinical COVID-19 onset by 94 to 95%, for which the elicited SARS-CoV-2-neutralizing antibodies are apparently directly responsible. Here, we demonstrate that highly neutralizing effect-confirmed convalescent plasmas significantly reduce the viral titers in the lung of SARS-CoV-2-infected Syrian hamsters and block the development of virally induced lung lesions. The present data provide a proof of concept that the presence of highly neutralizing antibody in COVID-19 convalescent plasmas is

Editor Kanta Subbarao, The Peter Doherty Institute for Infection and Immunity

Address correspondence to Hiroaki Mitsuya, hmitsuya@hosp.ncgm.go.jp.

The authors declare no conflict of interest.

Received 20 September 2021
Accepted 9 November 2021
Accepted manuscript posted online 24 November 2021
Published 23 February 2022

directly responsible for the reduction of viral replication and support the use of highly neutralizing antibody-containing plasmas in COVID-19 therapy with convalescent plasmas.

KEYWORDS COVID-19, SARS-CoV-2, convalescent plasma therapy, Syrian hamster COVID-19 model

More than a year had passed since the World Health Organization (WHO) declared a state of emergency, but the pandemic of the novel coronavirus (severe acute respiratory syndrome coronavirus 2 [SARS-CoV-2]) disease (COVID-19) is still spreading worldwide (1, 2). More than 215 million people have been infected, and more than 4.5 million lives have been lost as of 1 September 2021 (https://covid19.who.int/); COVID-19 is continuously posing the most serious public health and socioeconomic problem globally in this century (3). Vaccination is one of the most effective prophylactic health measures (4, 5) and is considered one of the most promising key strategies for curbing the current pandemic (6). Multiple COVID-19 vaccines, such as mRNA vaccines, BNT162b2 (7) and mRNA-1273 (8), and an adenovirus vector, ChAdOx1 nCoV-19/AZD1222 (9) and Ad26.COV2.S (10), are presently available in the United States, the European Union, and other parts of the world. Different classes of vaccines, such as inactivated COVID-19 vaccines, BBIBP-CorV (11), and CoronaVac (12), have now been approved for use by the WHO. Also, a recombinant protein nanoparticle vaccine, NVX-CoV2373 (13); a virus-like particle vaccine, plant-based VLP (14); a DNA vaccine, ZyCoV-D (15); and more than 130 vaccine candidates are currently under development (https://covid19.trackvaccines.org/). Yet how long the observed efficacy of vaccines lasts and whether such vaccines are effective in treating already-infected individuals remain to be determined (16). In addition, the spread of SARS-CoV-2 variants, which resist the efficacy of certain vaccines throughout the world, has been of great concern (17, 18).

Moreover, in terms of disease management, remdesivir (19), dexamethasone (20), baricitinib (21), and the interleukin 6 (IL-6) pathway inhibitors (e.g., tocilizumab) (22) are the only recommended agents for severely ill patients with COVID-19, although the efficacy of such agents is limited (23, 24). In terms of passive neutralizing activity treatment, not all monoclonal antibodies active against SARS-CoV-2 have proven to be clinically beneficial. Although bamlanivimab reportedly accelerated the natural decline in viral load in outpatients with COVID-19 (25), no benefit was demonstrated in a randomized controlled trial with the antibody in hospitalized patients (26), and the distribution of bamlanivimab and etesevimab together and etesevimab alone was paused in June 2021 in the United States. On the other hand, combination therapy with two potently SARS-CoV-2-neutralizing monoclonal antibodies, casirivimab and imdevimab, was reported to reduce 28-day mortality among patients in an open-labeled randomized trial (27) and has been authorized by the U.S. Food and Drug Administration for emergency use. Another investigational SARS-CoV-2-neutralizing monoclonal antibody, sotrovimab, has also been shown to be effective and is now available for emergency use for those at risk for progression to severe COVID-19 (28). Although a limited number of agents with known or putative antiviral or immunomodulating effects have been proposed for treating COVID-19, such agents, in many cases, have insufficient evidence of *in vitro* anti-SARS-CoV-2 activity or clinical benefit (29). In this regard, certain SARS-CoV-2-specific experimental agents have been reported, such as inhibitors of main protease (Mpro) (30–33) and RNA-dependent RNA polymerase (34) of the virus. However, it would take a few years and more likely longer until such virus-specific therapeutics become available in the clinical setting, although it is stressed that both effective vaccines and antiviral therapeutics are required for halting and possibly ending the current pandemic. In this regard, immunotherapies for certain cancers and autoimmune disorders are relatively well established (35); however, there are only a few immunotherapies for infectious diseases which were shown to be efficacious. The efficacy of plasma infusions of SARS-CoV-1-convalescent plasma is controversial mainly because most clinical trials were not controlled or randomized (36). Moreover, in many clinical trials, plasmas administered were not examined for their titers of neutralizing

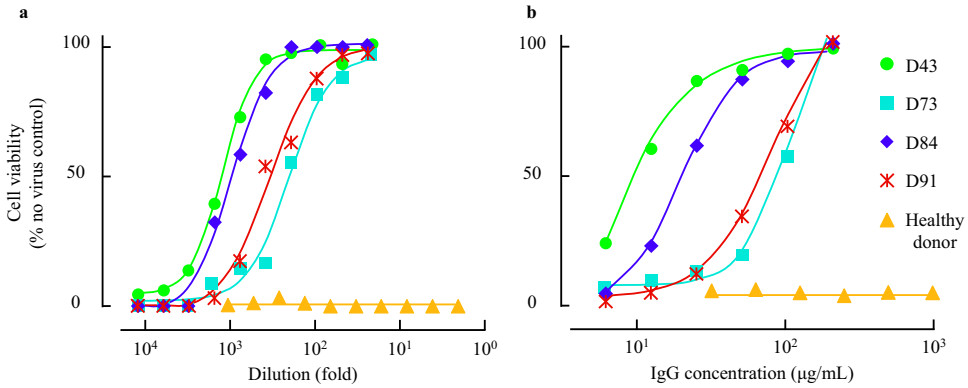

FIG 1 Antiviral activity of convalescent plasma and purified IgG. VeroE6^{TMPRSS2} cells were exposed to SARS-CoV-2$^{05\text{-}2N}$ with or without various concentrations of diluted plasma (a) or purified IgG (b). Note that highly neutralizing plasma (*hn*-plasma), D43 and D84, were highly potent, while moderately neutralizing plasma (*mn*-plasma), D73 and D91, were relatively moderately active against the virus. A plasma sample from a healthy and qRNA-PCR- and ELISA-confirmed SARS-CoV-2-uninfected individual and its IgG fraction failed to show significant CPE-blocking activity.

antibodies contained. Of note, fatality/clinical outcomes among those with COVID-19 receiving convalescent plasma whose titers of anti-SARS-CoV-2 receptor-binding domain (RBD) antibodies have been reportedly lower than in those receiving no plasma (37, 38), especially when such plasmas were administered early after the onset. The outcomes of those receiving high-titer anti-SARS-CoV-2-RBD or anti-SARS-CoV-2-spike antibodies early after the onset have also been shown to be favorable (37).

Imai and his colleagues have recently reported that SARS-CoV-2 efficiently replicates in the lungs of Syrian hamsters and causes severe pathological lung lesions that share characteristics with lung lesions in patients with COVID-19 (39). Here, we examined the efficacy of neutralizing activity-confirmed COVID-19 convalescent plasmas and such plasma-derived IgG fractions by employing the SARS-CoV-2-exposed transmembrane protease serine subtype 2 (TMPRSS2)-overexpressing VeroE6 (VeroE6^{TMPRSS2}) cells (30) and Syrian hamster model. The present data strongly suggest that the treatment of COVID-19 patients using highly neutralizing activity-confirmed convalescent plasmas would efficiently block the development of COVID-19-associated lung lesions.

RESULTS

COVID-19 convalescent plasma-derived IgG fractions block SARS-CoV-2 infection *in vitro*. We have previously examined the presence and temporal changes of the neutralizing activity of IgG fractions from 43 COVID-19 convalescent plasmas using cell-based assays (40). In the current study, we chose 2 highly neutralizing plasma (*hn*-plasma) samples and IgG fractions from donor 043 (D43) and D84, which were in the best 1.4 and 0.5% of 340 neutralizing activity-determined convalescent plasmas, respectively, and 2 moderately neutralizing plasma (*mn*-plasma) samples and IgG fractions from D73 and D91, which showed the top 40.5 and 20.9% neutralizing activity in the 340 convalescent plasmas, respectively, and we confirmed their activity to block the cytopathic effect (CPE) of a SARS-CoV-2 strain (SARS-CoV-2$^{05\text{-}2N}$) using VeroE6^{TMPRSS} cells and the methyl thiazolyl tetrazolium (MTT) method (30, 40). Figure 1 shows that all the four representative COVID-19 convalescent plasmas and IgG samples significantly blocked the CPE of SARS-CoV-2$^{05\text{-}2N}$. D43 and D84 plasmas were highly potent against the virus, with 50% inhibitory concentration (IC_{50}) ± standard deviation (SD) values of 1,400 ± 240-fold and 1,100 ± 60-fold, respectively, while D73 and D91 samples showed relatively moderate activity, with IC_{50} ± SD values of 220 ± 30 and 400 ± 90-fold, respectively (Fig. 1a and Table 1). IgG fractions purified from D43 and D84 plasmas also exerted potent activity, with IC_{50} ± SD values of 9.2 ± 1.3 and 9.8 ± 2.7 μg/ml, respectively, while those from D73 and D91 showed moderate activity, with IC_{50} ± SD values of 47.9 ± 9.0 and 24.9 ± 3.1 μg/ml, respectively (Fig. 1b and Table 1). A plasma sample from a healthy and quantitative RNA-PCR (qRNA-PCR)- and enzyme-linked immunosorbent

TABLE 1 Neutralizing activity of convalescent plasma and purified IgG (mean ± SD)[a]

Sample	Plasma IC_{50} (fold)	Purified IgG IC_{50} (μg/ml)	Anti-S1 IgG (%)
D43	1,400 ± 240	9.2 ± 1.3	140
D73	220 ± 30	47.9 ± 9.0	34
D84	1,100 ± 60	9.8 ± 2.7	100
D91	400 ± 90	24.9 ± 3.1	57
Healthy donor	<2	>1,000	<0.3

[a]Neutralizing activity of COVID-19 convalescent plasmas and their IgG fractions were determined using MTT assay employing VeroE6^{TMPRSS2} cells. The relative amounts of anti-SARS-CoV-2-S1-binding antibody were quantified using anti-SARS-CoV-2-S1 IgG ELISA with serially diluted D84 plasma samples for standardization. All the convalescent plasma and purified IgG showed various potency of neutralizing activity, while healthy donor plasma and its purified IgG were inert against SARS-CoV-2$^{05\text{-}2N}$. Of note, D43-derived plasma and purified IgG showed the most potent antiviral activity, with IC_{50} values of 1,400 ± 240-fold and 9.2 ± 1.3 μg/ml, respectively.

assay (ELISA)-confirmed SARS-CoV-2-uninfected individual and its IgG fraction failed to show significant CPE-blocking activity (Fig. 1 and Table 1). We have also quantified the amounts of SARS-CoV-2-S1-binding antibodies in each plasma sample by using D84 plasma as a reference (100%), employing a commercially available ELISA kit. D43, D73, and D91 contained 140, 34, and 57% of IgG relative to D84 plasma, respectively (Table 1), showing that the amounts of S1-binding antibodies contained in plasma samples were roughly proportionate to the blocking effects of each plasma and IgG fraction, although it is of note that the presence of greater amounts of S1-binding antibodies in plasma does not necessarily predict the presence of greater levels of neutralizing activity (40). Taken together, these data show that all the plasma samples used were highly or moderately active in blocking the infectivity and replication of SARS-CoV-2 and that the IgG fractions isolated from plasmas were largely responsible for the activity of plasmas to block the infectivity and CPE of the virus.

Body weight gains in SARS-CoV-2$^{UT\text{-}NCGM02}$-exposed and neutralizing plasma-receiving Syrian hamsters were significantly greater than those in control plasma-receiving animals. We have previously demonstrated that SARS-CoV-2 isolates efficiently replicate in the lungs of Syrian hamsters, causing severe pathological lung lesions (39). Such SARS-CoV-2-infected 7- to 8-month-old hamsters also underwent substantial weight loss by day 7 postinfection and continued to lose weight for up to 14 days postinfection (39). In the present study, we employed 1-month-old hamsters and intranasally inoculated them with 10^3 PFU of a clinically isolated SARS-CoV-2, SARS-CoV-2$^{UT\text{-}NCGM02}$ (set as day 0). In the 24 h following the inoculation (on day 1), three hamsters per group were intraperitoneally administered with 2 ml of plasma from a qRNA-PCR- and-ELISA-confirmed SARS-CoV-2-uninfected healthy individual (control plasma; see the protocol in Fig. S1 in the supplemental material). As the body weights of the control plasma-receiving hamsters (n = 3) were followed up every day, their weights continued to decrease by day 8 following the viral exposure, while the weights started to gain by day 9 and continued to gain thereafter. However, in hamsters that received the *hn*-plasma samples (D43 and D84), the decrease in body weights by day 8 was much less than in control plasma-receiving hamsters, and their body weights started to increase on day 9 and beyond (P values of the temporal changes in the body weights for the D43- and D84-receiving hamster groups to the control group were 0.0095 and 0.0092, respectively). One of the D73 plasma-receiving hamsters (hamster 28) had a significantly greater body weight decrease among the four D73 plasma-receiving hamsters, and the average body weights became close to those in the control plasma-receiving hamsters (Fig. 2) (the P value for the D73 plasma-receiving hamsters compared to four control plasma-receiving hamsters was 0.2025).

SARS-CoV-2$^{UT\text{-}NCGM02}$-exposed and neutralizing plasma-receiving Syrian hamsters develop less severe pneumonia. SARS-CoV-2-infected Syrian hamsters undergo lung injuries, which share characteristics with injuries seen in the lungs of SARS-CoV-2-infected individuals, including severe, bilateral, largely peripherally distributed, multilobular ground-glass opacity (GGO) lesions and lobular consolidations as examined using microcomputed tomographic (micro-CT) imaging (Fig. 3) (39). In order to examine the effects of administering neutralizing human plasmas on the development of

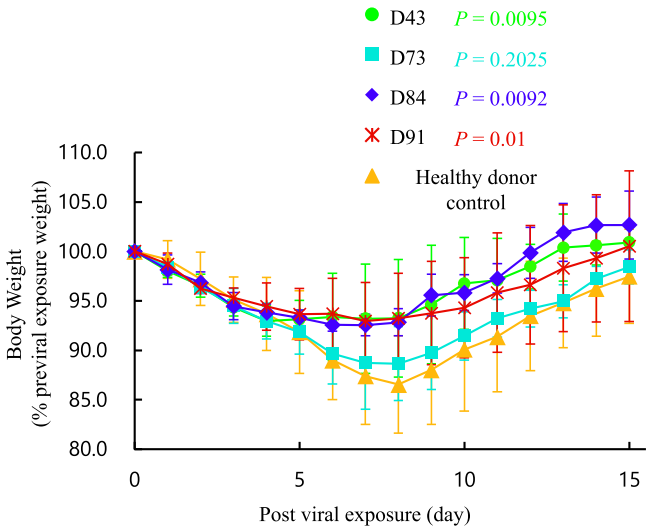

FIG 2 Body weight change in SARS-CoV-2-infected Syrian hamsters with plasma transfusion. Syrian hamsters were intranasally inoculated with 10^3 PFU of clinically isolated SARS-CoV-2 (SARS-CoV-$2^{UT\text{-}NCGM02}$). In 24 h following the inoculation, hamsters were intraperitoneally administered with 2 ml of convalescent plasma or a qRNA-PCR- and-ELISA-confirmed SARS-CoV-2-uninfected healthy individual-derived control plasma, and the body weight was monitored daily for 15 days. The mean relative value from the previral exposure baseline and SD values are shown. All the hamsters lost their weight by day 8 following the viral exposure, while the weights started to gain by day 9 and continued to gain thereafter. *P* values of the body weight change in D43-, D73-, D84-, and D91-receiving hamster groups compared to the control group were 0.0095, 0.2025, 0.0092, and 0.01, respectively.

SARS-CoV-2-induced lung lesions in virus-exposed Syrian hamsters, we employed the *in vivo* X-ray micro-CT image capturing in the present study. In all three SARS-CoV-$2^{UT\text{-}NCGM02}$-exposed hamsters, which intraperitoneally received 2 ml of the control plasma on day 1 postinfection (hamsters 21, 22, and 23), low-level infiltration with GGOs in bilateral lower lobes appeared by day 4 in both coronal and axial micro-CT thorax images (Fig. S2, open arrowheads). By day 6, those lesions evolved into a mixed pattern of GGOs, consolidations, and interlobular septal thickening seen in whole lung. By day 8, such lesions further worsened to show GGOs with consolidations and fibrous stripes in bilateral lung accompanied with mediastinal emphysema (shown with arrows), traction bronchiectasis, interlobular septal thickening, and/or cavitations (Fig. S2). Micro-CT scans taken on day 10, however, showed healing of the lung cavitation and mediastinal emphysema together with reduced GGOs. Micro-CT scans on day 12 show further healing of the consolidation and GGOs, while multiple focal fibrous stripes remained in the bilateral peripheral field (Fig. S2).

However, in all three hamsters that intraperitoneally received either of the two *hn*-plasma samples (hamsters 24, 25, and 26 received 2 ml of D43 plasma, while hamsters 30, 31, and 32 received 2 ml D84 plasma), no such extensive lung lesions developed throughout the 12-day period of observation, and the difference between the lung images of D43 and D84 plasma-receiving hamsters and those of control plasma-receiving hamsters 21, 22, and 23 on day 8 postinfection (the dorsal lung images of control plasma-receiving hamsters were taken from Fig. S2) was readily noticeable.

The lung micro-CT scan images of *mn*-plasma-receiving hamsters (hamsters 27, 28, and 29 received D73 plasma, while hamsters 33, 34, and 35 received D91 plasma) showed mixed but moderate GGO lesions and interlobular septal thickening in whole lung; however, no mediastinal emphysema or traction bronchiectasis was observed except in hamster 28 (Fig. 3a). Coronal micro-CT scan images confirmed the moderate changes in the lung scan images of those hamsters compared to the lung CT images of the control plasma-receiving hamsters (Fig. 3b).

D43 plasma administration apparently inhibited the spread of viral infection from bronchiolar to alveolar regions. On day 4 postinfection (on day 3 post-plasma administration), histopathological features and virus distribution patterns in the lung tissues of each hamster were examined. All histopathology and immunohistochemistry

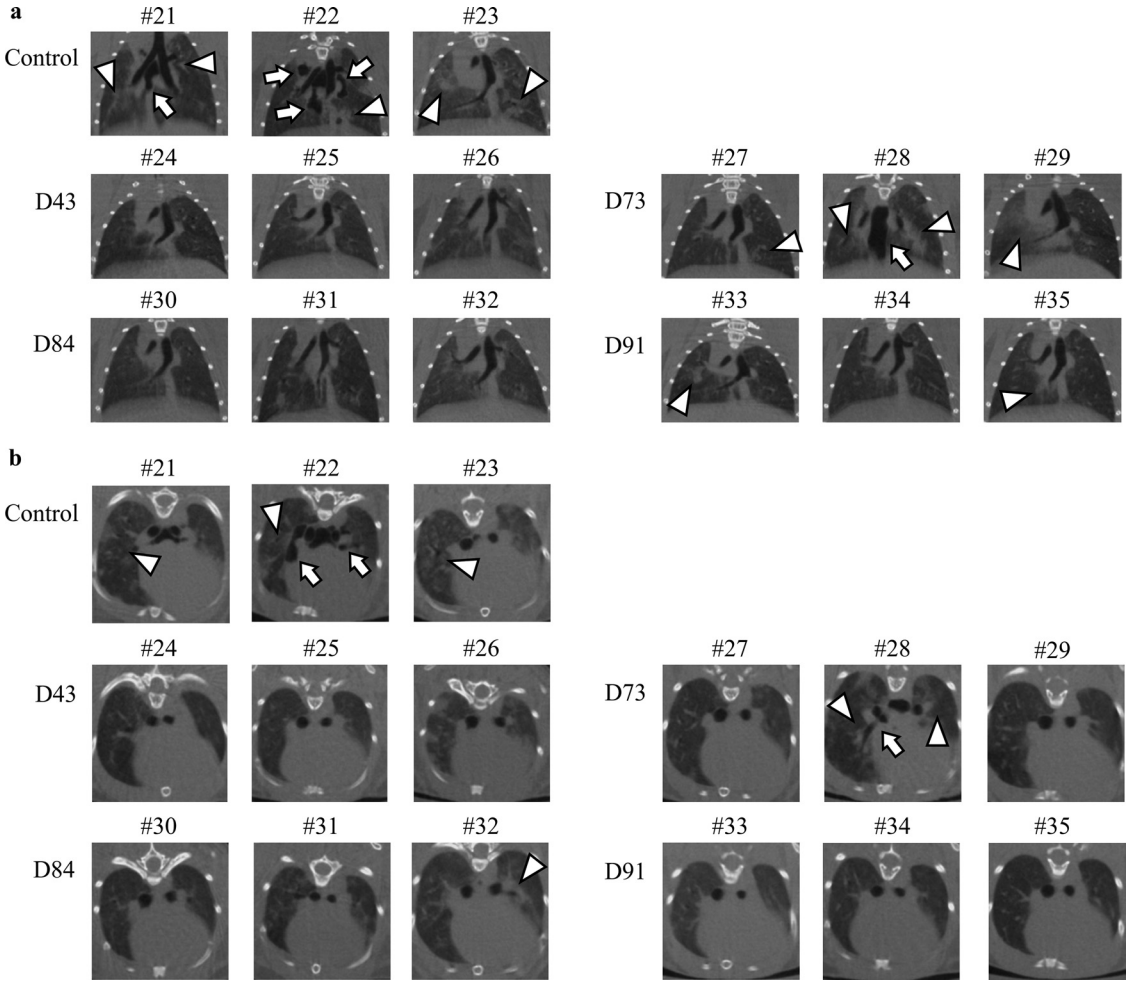

FIG 3 Micro-CT imaging of the lungs of SARS-CoV-2-infected Syrian hamsters with convalescent plasma transfusion on 8 days post-viral exposure. Coronal (a) and axial (b) images of the thorax of hamsters receiving the SARS-CoV-2 inoculation and COVID-19 convalescent plasma i.p. transfusion. (a and b) Control plasma-receiving hamsters (hamsters 21, 22, and 23) developed the ground-glass opacities (GGOs) with consolidations and fibrosis. However, in all three hamsters receiving *hn*-plasma (D43 for hamsters 24, 25, and 26 and D84 for hamsters 30, 31, and 32), no such lung abnormalities were observed throughout the 12 days of micro-CT imaging in hamsters 24, 25, and 30, and mild to moderate GGO and interlobular septal thickening were focally observed in hamsters 26, 31, and32. On the other hand, the chest CT images in *mn*-plasma-receiving hamsters (D73 for hamsters 27, 28, and 29 and D91 for hamsters 33, 34, and 35) showed mixed but moderate GGO lesions and interlobular septal thickening in whole lung; however, no mediastinal emphysema or traction bronchiectasis were observed except in hamster 28. Open arrowheads and arrows point to GGOs and mediastinal emphysema, respectively.

features obtained are illustrated in Fig. S3. Histopathology of the lung sections of each animal showed moderate inflammatory cell infiltration consisting of neutrophils, monocytes/macrophages, and lymphocytes around the bronchi and bronchioles. In some regions, inflammatory cells were detected in the alveoli. However, the degrees of histopathological changes substantially varied among hamsters, and there was no readily significant difference among the groups administered with different plasmas (Fig. 4a, c, e, g, and i and Fig. S3a to e). Then, immunohistochemistry with anti-SARS-CoV-2 antibody revealed viral antigens in the bronchiole epithelium and viral spreading to the alveolar epithelium surrounding the bronchioles in all the animals except for D43 plasma-receiving hamsters. Notably, in the D43-receiving animals (Fig. 4d and Fig. S3b), substantially fewer viral antigens were seen, and the extent of the viral spreading was apparently limited to bronchial and alveolar epitheliums adjacent to bronchioles regardless of the degrees of histopathological changes compared to the amounts of viral antigens seen in the lungs of control plasma- and D73, D84, and D91 plasma-receiving hamsters (Fig. 4b, f, h, and j and Fig. S3a, c, and d). Moreover, the numbers of viral antigen-positive cells in the alveolar

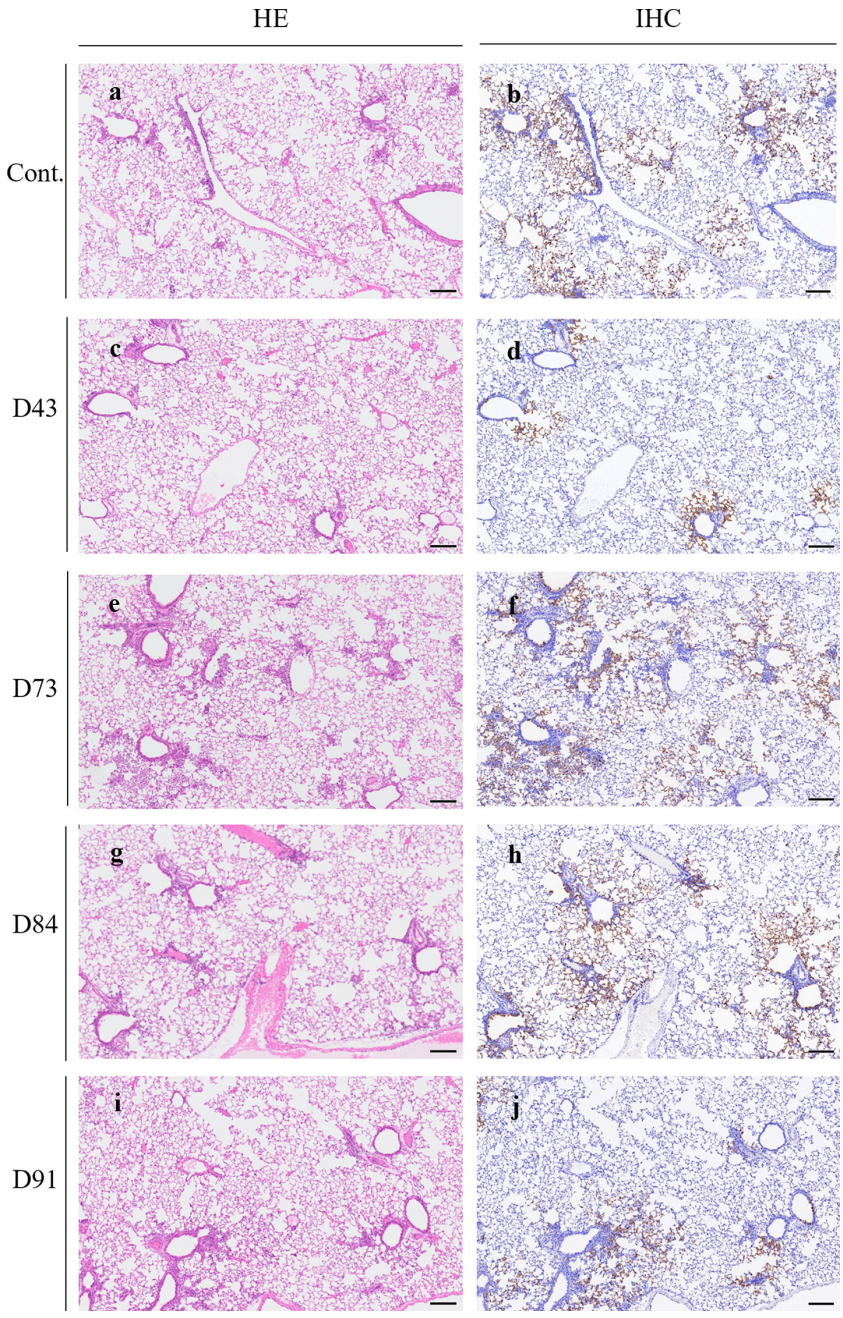

FIG 4 Pathological examination of the hamsters treated with plasma. Representative images of histopathology and immunohistochemistry on the lung sections of hamsters treated with control or each plasma on day 1 postinfection are shown. Hematoxylin and eosin (H&E) staining of the lung sections obtained from the control animals (a) and plasma D43- (c), D73- (e), D84- (g), or D91-treated (i) animals. Immunohistochemistry (IHC) for SARS-CoV-2 antigen detection of the lung sections obtained from the control animals (b) and plasma D43- (d), D73- (f), D84- (h), or D91-treated (j) animals. Scale bar, 200 μm.

regions also appeared less in the lung of D43 plasma-receiving hamsters (Fig. 4d and Fig. S3b) than in the control plasma-receiving and D73, D84, or D91 plasma-receiving animals (Fig. 4b, f, h, and j and Fig. 3a, c, and d).

Neutralizing activity-confirmed plasmas significantly suppressed the replication of SARS-CoV-2 in the lung of hamsters. All the neutralizing activity-confirmed COVID-19 convalescent plasma samples (D43, D73, D84, and D91 plasmas) mitigated the body weight reduction and SARS-CoV-2-induced lung lesions (Fig. 2 and 3; Fig. S2); however, the histopathological examination and immunostaining method largely failed to

detect differences in the presence or spread of the virus between the hamsters receiving the control plasma and those receiving neutralizing activity-confirmed plasmas (Fig. 4 and Fig. S3). Thus, we attempted to quantify the amounts of infectious virions in the lungs of hamsters receiving control plasma or D43, D73, D84, or D91 plasmas. Each hamster was exposed to the virus on day 0, intraperitoneally administered with 2 ml of each plasma on day 1, and sacrificed on day 4. Thereafter, each lung was homogenized and the virus titers in the homogenates were determined employing plaque-forming assays using VeroE6^{TMPRSS2} cells. As shown in Fig. 5a, the geometric mean titer for the hamsters receiving control plasma was $10^{8.5}$ PFU/g, while the administration of D43 and D91 plasmas had significantly suppressed the replication of SARS-CoV-2$^{UT\text{-}NCGM02}$ with viral titers of down to $10^{7.0}$ ($P = 0.0003$) and $10^{7.7}$ ($P = 0.037$) PFU/g, respectively, while the reductions by D73 and D84 plasmas were not statistically significant ($P > 0.05$; Fig. 5a). When IgG fractions isolated from plasmas were intraperitoneally administered to hamsters, the D43 IgG fraction gave the greatest reduction with a geometric mean infectious viral titer of $10^{7.1}$ PFU/g compared to the viral titer in the control plasma-receiving hamsters with a geometric mean titer of $10^{8.4}$ PFU/g, while D91, D84, and D73 IgG fractions gave mean titers of $10^{7.7}$ ($P = 0.015$), $10^{7.8}$ ($P = 0.037$), and $10^{8.0}$ ($P > 0.05$) PFU/g, respectively (Fig. 5b). It has recently been reported that the systemic monoclonal human-neutralizing antibody administration in Syrian hamsters effectively blocks the SARS-CoV-2 infection in lung but not in nasal turbinate (41). In this regard, we also determined the viral titer in nasal turbinate tissues in the convalescent plasma-administered SARS-CoV-2-infected Syrian hamsters. As shown in Fig. 5c, the geometric mean viral titer for the hamsters receiving control plasma was $10^{7.9}$ PFU/g, while the administration of D84 and D91 plasmas had significantly more deeply suppressed the replication of SARS-CoV-2$^{UT\text{-}NCGM02}$ with viral titers of $10^{7.0}$ ($P = 0.010$) and $10^{7.2}$ ($P = 0.037$) PFU/g, respectively, while the reductions by D43 and D73 plasmas were not statistically significant ($P > 0.05$) (Fig. 5c). On the other hand, when the IgG fraction was administered to hamsters, the geometric mean viral titers in nasal turbinate in D43, D73, D84, and D91 IgG-receiving hamsters were $10^{7.1}$, $10^{7.4}$, $10^{7.5}$, and $10^{7.5}$ PFU/g, respectively, which were not statistically significant compared to the values in the control IgG-receiving hamsters ($P > 0.05$) (Fig. 5d). The complete failure of purified IgG fractions to block the replication of the virus in nasal turbinate tissues (Fig. 5d), despite that viral replication was blocked by plasma administered (Fig. 5c), may have resulted from the administration of relatively fewer amounts of purified IgG than the amounts of plasma administered. In fact, as shown in Table S2, the equivalent amounts of plasma are all less than the amounts of purified IgG amounts administered by 10% to 30%. Considering that the same amounts of purified IgG effectively blocked the replication of the virus in the lung (Fig. 5b), the present data are in line with the findings by Zhou et al. (41) and Haagmans et al. (42) that SARS-CoV-2 replication is more susceptible to the SARS-CoV-2-blocking effect of monoclonal antibodies or convalescent plasma samples in lungs than in nasal turbinate.

In an attempt to see the effects of administering IgG fractions isolated from neutralizing human plasmas on the development of lung lesions in virus-exposed animals, we conducted an additional histopathological and immunostaining study. Since we had failed at identifying the difference in the histopathological findings among lungs of hamsters receiving various plasmas, we examined the lung in one hamster which had the lowest infectious viral titer among each group ($n = 4$) in this additional study. Representative images of the immunostained lung sections of hamsters showed that the infected cells are observed from the terminal bronchioles into the alveolar region in animals treated with control plasma IgG, IgG from D73, D84, and D91 plasmas; however, the number of infected cells was much less in the terminal bronchioles and alveolar regions in the hamster receiving IgG fraction from D43 plasma (Fig. S4), corroborating the histopathological and immunostaining observations in hamsters receiving plasmas (Fig. 4).

COVID-19 convalescent plasmas variably contain antibodies that specifically bind to viral components. We finally attempted to determine which antibodies within the four convalescent D43, D73, D84, and D91 plasma samples bind to SARS-CoV-2 components using the Jess capillary-based Western blotting system. The four viral

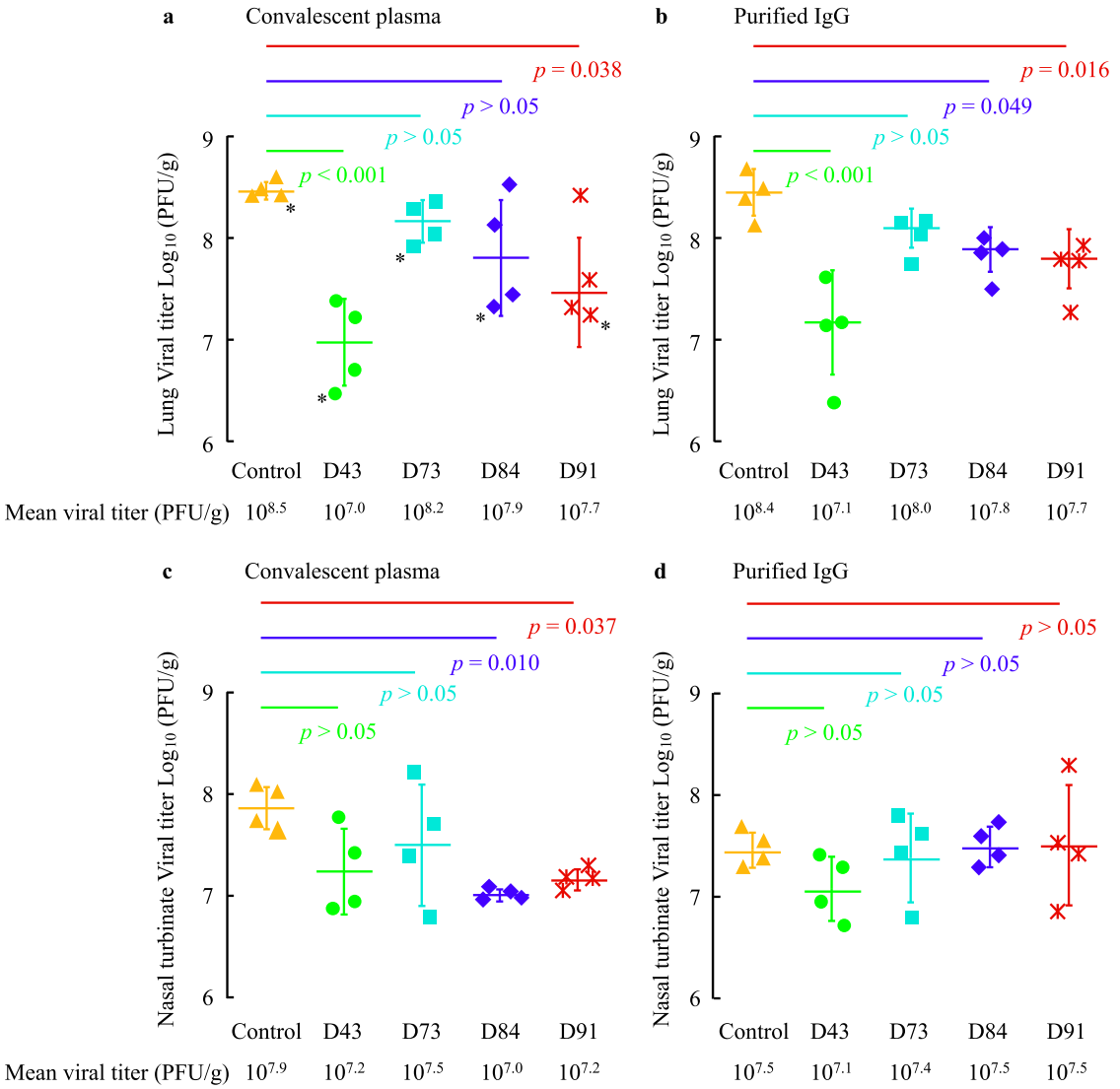

FIG 5 Neutralizing activity of convalescent plasma in the lungs and nasal turbinate of SARS-CoV-2-infected Syrian hamsters with plasma transfusion. Syrian hamsters were intranasally inoculated with 10^3 PFU of clinically isolated SARS-CoV-2 (SARS-CoV-$2^{UT\text{-}NCGM02}$). In 24 h following inoculation, hamsters were intraperitoneally administered with 2 ml of plasma (a and c) or plasma-derived purified IgG (b and d). Four Syrian hamsters per group were sacrificed on 4 days post-viral exposure (3 days post-plasma transfusion), and the virus titers in the lungs (a and b) and nasal turbinate (c and d) were determined by employing $VeroE6^{TMPRSS2}$ cells. The geometric mean titer and SD values are shown.

components (RBD, S1, S2, and nucleocapsid [NC]) are covalently fixed to the capillary, and the presence of human IgG specifically bound to each viral component in the capillary is detected by exposing the capillary to horseradish peroxidase (HRP)-conjugated anti-human IgG and iridescent light elicited by luminol mediated by HRP. Figure 6a illustrates that each of the plasma contained IgG antibodies reactive with viral components, showing that the amounts and the ratios of each viral component-specific antibodies were substantially varied. Among the four convalescent plasma tested, D43, one of the two *hn*-plasmas, contained the largest amounts of anti-RBD, anti-S1, and anti-NC IgG, while D84 contained the largest amount of anti-S2 and anti-whole-spike IgG (Fig. 6b). Interestingly, the two *mn*-plasmas contained low levels of anti-RBD, anti-S1, anti-whole-spike, and anti-NC IgG.

DISCUSSION

Chan et al. reported that SARS-CoV-2 produces severe lung lesions in Syrian hamsters, as in humans, at least in part because the amino acid sequences of angiotensin-converting enzyme 2 (ACE-2) that interact with the RBD of SARS-CoV-2-S1 are in high identity and target cells in

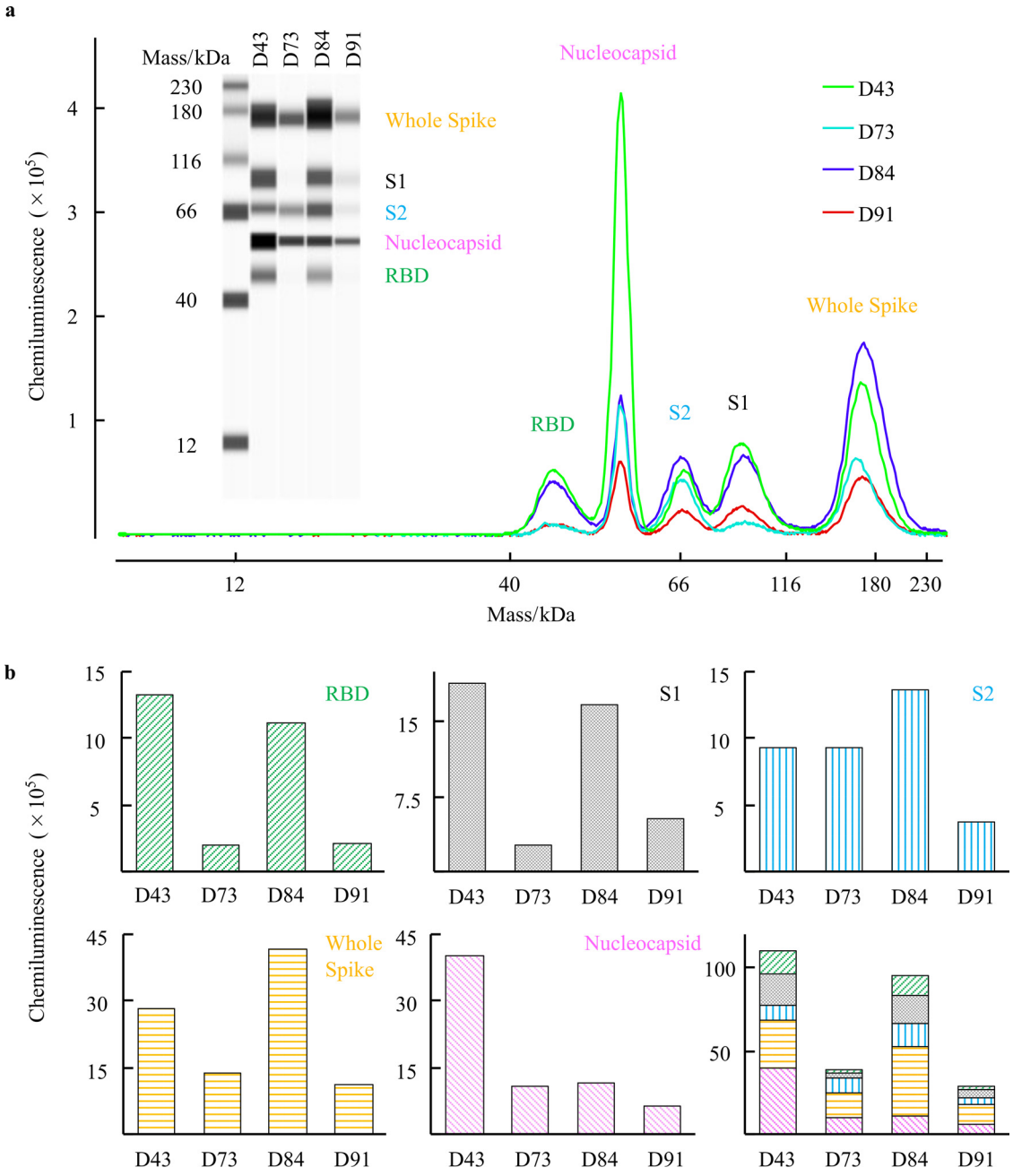

FIG 6 Characteristics of the anti-SARS-CoV-2 IgG in convalescent plasma against multiple viral components. The anti-SARS-CoV-2 IgG in each COVID-19 convalescent plasma reactive against SARS-CoV-2 viral components (RBD, S1, S2, whole spike, and nucleocapsid [NC]) was detected using the Simple Western Jess system. (a) Western blotting image obtained with the Jess system and the immunoreactive signals for the presence of viral components bound by anti-SARS-CoV-2 IgG by using Simple Western Jess System. All four COVID-19 convalescent plasmas contained the SARS-CoV-2-specific IgG. (b) Quantification of IgG levels in four COVID-19 convalescent plasmas. D43 and D84 plasma samples had large amounts of anti-RBD IgG, while D73 and D91 had much lower amounts of anti-RBD IgG. The same trend was seen in the amounts of anti-S1 and anti-whole-spike IgGs. On the other hand, the D43 sample had a smaller amount of anti-S2 IgG than D84. D43 had a much larger amount of anti-NC IgG than D73, D84, and D91.

both hamsters and humans are effectively infected with the same virus (43). Chan et al. also demonstrated that convalescent-phase sera from SARS-CoV-2-infected hamsters effectively reduced the replication of the virus in SARS-CoV-2-inoculated animals as assessed by qRNA-PCR and immunohistochemistry (43). Further, Haagmans et al. reported that the administration of neutralizing activity-confirmed human convalescent plasma (*hn*-plasma) or SARS-CoV-2-neutralizing human monoclonal antibody effectively protected Syrian hamsters from the occurrence of SARS-CoV-2-induced lung lesions when the animals were prophylactically (24 h

prior to the viral inoculation) treated, while the diluted *hn*-plasma failed to show such protective effects (42). In the present study, we extended the observations by groups, including Chan et al. and Haagmans et al., and demonstrated that *hn*-plasmas reduced the severity of lung lesions in SARS-CoV-2-exposed Syrian hamsters even when such plasmas were given to the animals 24 h after the inoculation compared to those receiving a nonneutralizing (control) plasma or moderately neutralizing plasmas (*mn*-plasmas) as assessed with micro-CT-captured images (Fig. S2 in the supplemental material and Fig. 3) and the presence of SARS-CoV-2-infected cells in the lung (Fig. 4 and Fig. S3 and S4). In fact, there is a growing body of literature that convalescent plasma therapy is not beneficial when started in the late stage of the disease (44), and early transfusion (within 3 days of hospital administration) of *hn*-plasma represents the optimal use for the highest efficacy of the treatment (45).

Moreover, *hn*-plasmas induced a significant reduction of viral titers in the lungs of SARS-CoV-2-exposed Syrian hamsters compared to those receiving control plasma or *mn*-plasmas (Fig. 5a). IgG fractions purified from *hn*-plasmas also substantially reduced viral titers in the lungs of hamsters (Fig. 5b). In the current study, although the administration of *hn*-convalescent plasma significantly suppressed the development of lung lesions and viral replication in lung, it was less effective in blocking viral replication in nasal turbinate (Fig. 5). In this regard, it was thought that SARS-CoV-2 replication is more susceptible to the neutralization by monoclonal antibodies or convalescent plasma samples in lungs than in nasal turbinate (41, 42). It is also possible that the innate immune responses triggered by SARS-CoV-2 are tissue specific and differ between lung tissues and nasal mucosa. In this regard, the administration of convalescent plasma, but not purified IgG, may contribute to limited immune response in the upper respiratory tract. In fact, when human primary nasal turbinate and lung tissues/cells were exposed to SARS-CoV-2 *ex vivo*, robust antiviral and inflammatory innate immune responses reportedly occurred in nasal mucosa but not in lung tissues, suggesting limited innate immune response to SARS-CoV-2 in the lung (46). These data strongly suggest that administering *hn*-COVID-19 convalescent plasmas would be efficacious in treating patients with COVID-19, and *mn*-plasmas are unlikely to be effective in treating COVID-19 patients. The data also suggest that the IgG fractions largely contribute to the antiviral activity of *hn*-plasma, although other immune responses, such as CD8-positive ($CD8^+$) killer T-cell and Fc effector functions, may contribute to protection, and their relative importance in protection against COVID-19 is to be investigated (47, 48). We believe that the experimental conditions we employed in the current study are very close to the clinical situations in the case of SARS-CoV-2 infection. We also demonstrated that the IgG fraction purified from convalescent plasma is largely responsible for the observed protective effect of the convalescent plasmas.

Several recent clinical studies suggest that neutralizing antibodies are generally sufficient to confer protection against the SARS-CoV-2 infection and that the protection against COVID-19 development is largely explained by SARS-CoV-2-neutralizing antibody responses, leaving less room for impact of T cells on correlation. Yet the efficacy of infusions of COVID-19 convalescent plasma has been controversial, mainly because most clinical trials were not well controlled or randomized (36). However, the failure of most COVID-19 convalescent plasma infusion studies to prove to be efficacious is likely due to the conditions in which the plasmas used were not confirmed to contain high titers of neutralizing activity before transfusion. In fact, a few studies where only convalescent plasma whose levels of anti-SARS-CoV-2-RBD antibodies were confirmed to be high have produced favorable clinical results (37, 38).

It is noteworthy that even in the well-planned clinical studies where high titers of neutralizing antibodies were used, a number of such clinical studies employed different ways and means to express neutralizing activity, such as 50% neutralization titers, reciprocal neutralizing antibody titers, and IC_{50} $\log_{10}$ geometric mean titers. Moreover, such clinical studies have used different cells and viral strains in quantifying neutralizing activity of plasmas. Thus, establishing an "international unit" or "international standard" is being thought to be needed to compare across various studies and to calibrate the strength of neutralization with a reference human convalescent-phase sera

panel. Establishing such a standard should improve the correlation between the levels of neutralization activity and resulting clinical efficacy (49).

In our previous study (40), to possibly calibrate the neutralizing activity of COVID-19 convalescent plasmas with the neutralizing activity of plasmas determined in other studies, we used neutralizing unit per milligram protein of IgG derived from such COVID-19 convalescent plasmas. In the present study, from among 340 COVID-19 convalescent plasma samples we have examined for their neutralizing activity using SARS-CoV-$2^{05\text{-}2N}$ that was isolated in Tokyo in March 2020 and VeroE6^{TMPRSS} (2) cells as target cells as previously described (40), we chose four plasmas as references of SARS-CoV-2-neutralizing plasmas. The four plasma samples D43, D73, D84, and D91 were in the top 1.4%, 40.5%, 0.5%, and 20.9% of 340 COVID-19 convalescent plasma samples, respectively. It is of note that approximately 60% of convalescent plasmas have low or no significant neutralizing activity, as we mentioned in our previous report (40). The reason why potently neutralizing D43 most effectively blocked the infection and replication of the virus in hamsters, while the comparably neutralizing D84 was less effective in doing so in hamsters, is not clear. One possibility is that convalescent plasmas contain polyclonal neutralizing antibodies and their constituents may substantially vary from one convalescent plasma to another (50, 51). Thus, even if a plasma sample exerts potent neutralizing activity in a cell-based assay, its neutralizing activity may not be directly well reproduced in the bodies of hamsters where the virus may unevenly infect and replicate so that the efficacy may vary depending on the constituents of polyclonal neutralizing antibodies. Also, the virus used in the cell-based assays differed from the virus used for the animal study: the virus we used in the present cell-based assays was SARS-CoV-$2^{05\text{-}2N}$ (PANGO lineage B), but the virus we used for inoculation of the animals was SARS-CoV-$2^{UT\text{-}NCGM02}$ (PANGO lineage A).

One limitation of the current study is that only one SARS-CoV-2 strain (SARS-CoV-$2^{05\text{-}2N}$) was employed in our cell-based assays, and the results obtained here may not predict the efficacy in individuals infected with other SARS-CoV-2 strains, in particular, SARS-CoV-2 variants recently isolated (52–55), which may escape neutralizing antibodies in plasmas used in the present study (56) or may replicate more efficiently than previously isolated SARS-CoV-2 strains such as SARS-CoV-$2^{05\text{-}2N}$ (57). The two viral strains, SARS-CoV-$2^{UT\text{-}NCGM02}$ and SARS-CoV-$2^{05\text{-}2N}$, used in the current study were isolated from each of two COVID-19 patients in February and March 2020, respectively. We have determined the sequences of these two strains: SARS-CoV-$2^{UT\text{-}NCGM02}$ was of the PANGO lineage A, while SARS-CoV-$2^{05\text{-}2N}$ was of the PANGO lineage B. As for the viruses that infected the four individuals in early 2020, no variants of concern (VOCs) or variants of interest (VOIs) had been reported in Tokyo or elsewhere. However, since Global Initiative on Sharing All Influenza Data (GISAID) clade G variants that carry the spike-G614 mutation had been isolated in March 2020 and had become the major variant in Japan by April 2020 (58), some of the patients may have been infected with the spike-G614-carrying variants rather than with the wild-type, spike-D614-carrying virus.

The other limitation of the current study is the lack of cytokine/chemokine or prolonged period profile analysis. We previously reported that while the neutralizing activity of convalescent plasmas in patients with COVID-19 often wanes in a time-dependent manner, the amounts of anti-SARS-CoV-2-S1-binding IgG titer persist longer (40). However, unlike in humans, although Syrian hamsters infected with SARS-CoV-2 were reported to show a marked increase in cytokine/chemokine mRNA levels, especially in the acute phase of infection (2 to 4 days postinfection) (43), they generally completely recovered from the infection around day 8 following inoculation and beyond, despite that they develop significant pneumonia, probably indicating that the cytokine/chemokine storm would be less severe and less destructive than in humans.

As of this writing, no potent antiviral agents active against SARS-CoV-2 are available for the use of animal models. In this regard, the present study, for the first time, demonstrates that, even 1 day after the inoculation of SARS-CoV-2 to hamsters, highly neutralizing convalescent human plasmas and their IgG fractions effectively prevent the

occurrence of pneumonia and block viral replication in the lung. Based on the present data, we have started randomized clinical trials in February 2021 in which only highly neutralizing plasmas are administered to patients with SARS-CoV-2 infection at early stages of the disease. Also, it is of note that when promising small-molecule compounds are developed, the current hamster model in which treatment is begun following the establishment of SARS-CoV-2 infection should serve as one of the most suitable methods for determination of the efficacy of potential antiviral agents. In conclusion, the present data strongly suggest that administering *hn*-COVID-19 convalescent plasmas should be efficacious in treating patients with COVID-19, but potent neutralizing activity has to be confirmed before administering such convalescent plasmas.

MATERIALS AND METHODS

Patients. Four patients were enrolled in the present work who were diagnosed with COVID-19 in February to May 2020 and agreed to participate in the clinical studies (approval numbers NCGM-G-003472 and NCGM-G-003536) to donate convalescent plasmas (40). These four donors were recruited from other medical institutions when they were discharged from those institutions, where no isolation of SARS-CoV-2 strains was attempted. Donated plasmas were stored at −20°C until use.

Cells, viruses, and IgG purification. TMPRSS2-overexpressing VeroE6 (VeroE6^{TMPRSS2}) cells (RRID CVCL_YQ49) were obtained from the Japanese Collection of Research Bioresources (JCRB) Cell Bank (Osaka, Japan). VeroE6^{TMPRSS2} cells were maintained in Dulbecco's modified Eagle's medium (DMEM) supplemented with 10% fetal bovine serum, 100 μg/ml penicillin, 100 μg/ml kanamycin, and 1 mg/ml G418 under humidified atmosphere containing 5% CO_2 at 37°C. The two SARS-CoV-2 strains, SARS-CoV-2$^{UT\text{-}NCGM02}$ (PANGO lineage A, GISAID accession ID EPI_ISL_418809) (39) and SARS-CoV-2$^{05\text{-}2N}$ (PANGO lineage B) (40) were isolated in February and March 2020, respectively, in Tokyo, Japan, as previously described. IgG fractions were purified from convalescent plasma at Immuno-Biological Laboratories (Gunma, Japan) by using rProtein A Sepharose Fast Flow (Cytiva, Marlborough, MA) and eluted in phosphate-buffered saline (PBS). The IgG fractions were stored at −80°C until use.

Antiviral assays. The SARS-CoV-2-neutralizing activity of donated plasma and purified IgG was determined as previously described (30, 40, 59). In brief, VeroE6^{TMPRSS2} cells were seeded in 96-well flat microtiter culture plates at the density of 1×10^4 cells/well. On the following day, the virus (SARS-CoV-2$^{05\text{-}2N}$) was mixed to the various concentrations of the plasma or purified IgG fractions and incubated for 20 min at 37°C. The preincubated mixture was inoculated to the cells at a multiplicity of infection (MOI) of 0.01. The cells were cultured for 3 days, and the number of viable cells in each well was measured using Cell Counting Kit-8 (Dojindo, Kumamoto, Japan). The potency of SARS-CoV-2 inhibition by plasma or purified IgG was determined based on its inhibitory effect on virally induced cytopathicity in VeroE6^{TMPRSS2} cells. The amounts of SARS-CoV-2-S1-binding antibodies in each plasma sample were determined by using anti-SARS-CoV-2 ELISA (IgG) (Euroimmun, Lübeck, Germany). The total human IgG concentration was determined by using Human IgG ELISA Kit (Abcam, Cambridge, UK).

Experimental infection of Syrian hamsters. All of the animal infection experiments were conducted as previously described (39). In brief, 1-year-old male Syrian hamsters (Japan SLC Inc., Shizuoka, Japan) were enrolled. Hamsters were intranasally inoculated with 10^3 PFU (in 100 μl) of SARS-CoV-2$^{UT\text{-}NCGM02}$ under ketamine-xylazine anesthesia. On the following day, 2 ml of convalescent plasma (experiments 1 and 2) or purified IgG (experiment 3) were intraperitoneally (i.p.) transfused to each Syrian hamster (Fig. S1 in the supplemental material). The total dosage and the dosage per body weight of human IgG in 2 ml plasma are shown in Table S1. The total amounts of human IgG in purified IgG fraction transfused to hamsters and plasma equivalent are shown in Table S2. The hamsters were monitored until the designated endpoint of the experiments.

For experiment 1, to monitor the body weight change and the micro-CT image, three hamsters per group were enrolled. The daily body weight was monitored for 15 days, and micro-CT imaging was conducted on days 0, 4, 6, 8, 10, and 12 postinfection. The body weight was compared with the preinfection baseline, and the relative values were calculated. The changes in the body weights from the baseline of each hamster treated with plasma were compared, and *P* values were calculated. In experiments 2 (plasma administered i.p.) and 3 (purified IgG fraction administered i.p.) in order to determine the *in vivo* antiviral activity of the convalescent plasma or purified IgG, four hamsters per group were enrolled. Hamsters were sacrificed on the fourth day postinfection, and lungs were collected for histological examination and viral titration (Fig. S1). The viral titer in the lungs was determined by means of plaque assays in VeroE6^{TMPRSS2} cells. All experiments with hamsters were performed in accordance with the Science Council of Japan's Guidelines for Proper Conduct of Animal Experiments. The protocol was approved by the Animal Experiment Committee of the Institute of Medical Science, the University of Tokyo (approval number PA19-75).

Micro-CT imaging. The chest CT images of the SARS-CoV-2-infected hamsters were captured as previously described using an *in vivo* micro-CT scanner (CosmoScan FX; Rigaku Corporation, Japan) until 12 days postinfection under ketamine-xylazine anesthesia. The imaging was conducted under the following conditions: 2 min at 90 kV, 88 μA, field of view (FOV) of 45 mm, and pixel size of 90.0 μm. After scanning, the lung images were reconstructed by using the CosmoScan Database software (Rigaku Corporation) and analyzed as per the manufacturer's instructions.

Pathological examination. Excised animal tissues were fixed in 10% buffered formalin and processed for paraffin embedding. The paraffin blocks were cut into 3-μm-thick sections and then mounted on silane-coated glass slides. One section from each tissue sample was stained using a standard hematoxylin and eosin procedure; another was processed for immunohistochemistry. After deparaffinization, antigens were activated (121°C, 10 min) with Target Retrieval Solution, pH 6.0 (Dako Cytomation, Glostrup, Denmark), and endogenous HRP was inactivated by hydroperoxide treatment. The sections were treated with 5% normal goat serum for 30 min at room temperature and incubated with rabbit monoclonal anti-SARS-CoV nucleoprotein antibody (Sino Biological, Beijing, China) at 4°C overnight. Specific antigen-antibody reactions were visualized by means of 3,3′-diaminobenzidine tetrahydrochloride staining using the Dako Envision system (Dako Cytomation).

Detection and quantification of anti-SARS-CoV-2 IgG bound to viral components. The amounts of anti-SARS-CoV-2 IgG antibodies reactive with SARS-CoV-2 viral components in convalescent plasma were determined using the capillary electrophoresis Simple Western Jess apparatus and the SARS-CoV-2 Multi-Antigen Serology Module (Protein Simple, San Jose, CA) according to the manufacturer's instructions. In brief, various recombinant viral components (RBD [200 μg/ml], NC [5 μg/ml], S1 [20 μg/ml], S2 [20 μg/ml], and whole spike [20 μg/ml]) were covalently fixed with UV irradiation to a 12-230 kDa Jess & Wes Separation Module (Protein Simple) capillaries. The immobilized viral components were then exposed to each of 30-fold diluted convalescent plasma samplesf (primary antibodies). Subsequently, the antibodies bound to the viral components were probed with HRP-conjugated anti-human IgG (secondary antibody). The presence of human IgG in the module was detected by iridescent light produced by luminol reagent being mediated by HRP. The signal intensity was quantified and plotted as a peak graph in the analysis software, Compass for SW ver. 5.0.1 (Protein Simple), and visualized as a virtual Western blot-like image, which is similar to traditional Western blot images.

Statistical analysis. For the comparison of the temporal changes in body weights of hamsters receiving control and convalescent plasma (control, D43, D73, D84, and D91), the changes in the body weights relative to the body weight before viral exposure were modeled with quartic functions. This is because each curve has a minimum around the middle of the postinfection days and high values at both edges. Therefore, the number of parameters determined is five, and the function was fitted to the data by use of the nonlinear least-squares method, which was performed by the Levenberg-Marquardt algorithm. The F statistics for the comparisons of two curves of the body weight changes were calculated, and the *P* values were derived (60). The distribution of the residuals was tested and found to be consistent with normality. Because of the nonlinearity of the model, the *P* values are only approximate. For the viral titer in lung, each convalescent plasma receiving group was compared with the healthy donor plasma receiving group using Dunnett's test by using JMP Pro 15.0.0 (SAS Institute, Cary, NC).

SUPPLEMENTAL MATERIAL

Supplemental material is available online only.

SUPPLEMENTAL FILE 1, PDF file, 3.8 MB.

ACKNOWLEDGMENTS

This work was supported in part by the Japan Agency for Medical Research and Development (AMED) (grant numbers JP20fk0108160 and JP20fk0108502 to K.M.; JP19fk0108113, JP20nk0101612, JP19fm0108006, JP21wm0125002, JP20fk0108260, and JP20fk0108502 to Y.K.; and JP20fk0108502, JP20fk0108257, and JP20fk0108510 to H.M.), the MHLW Research on Emerging and Re-emerging Infectious Diseases and Immunization Program (grant number JPMH20HA1006 to K.M.), the National Center for Global Health and Medicine Research Institute (grant number 20A2003D to K.M.), the National Institutes of Allergy and Infectious Diseases (grant number HHSN272201400008C to Y.K.), and the Intramural Research Program of the Center for Cancer Research, National Cancer Institute, National Institutes of Health (H.M.). These funding sources were not involved in study design; collection, analysis, and interpretation of data; the writing of the report; or the decision to submit the paper for publication.

We are grateful to Miwa Tamura-Nakano and Chinatsu Oyama in the communal laboratory of NCGM Research Institute for their technical support. We also thank Mariko Kato for technical assistance. We thank all the patients who participated in the clinical trial for collection of convalescent plasma, and staff of the Diseases Control and Prevention Center, Center for Clinical Sciences, Department of Hematology, Clinical Laboratory Department, Department of Clinical Engineering, and Nursing Department at the National Center for Global Health and Medicine Hospital.

Conceptualization, Yuk.T, K.M., Y.K., and H.M.; Methodology, Yuk.T., Ma.I., K.M., N.N., Y.K., and H.M.; Formal Analysis, K.O.; Investigation, Yuk.T., Ma.I., K.M., N.N., N.H.-K., K.I.-H., Mu.I., M.K., T.M., and Yui.T.; Data Curation, Yuk.T., Ma.I., K.M., K.I.-H, Mu.I., M.K., and T.M.;

Writing – Original Draft, Yuk.T. and H.M.; Writing – Review & Editing, Ma.I., N.N., N.H.-K., Yui.T., K.O., T.S., and Y.K.; Supervision, T.S., Y.K., and H.M.; Project Administration, H.M.; Funding Acquisition, K.M., Y.K., and H.M.

We declare that we do not have any competing interests related to this study.

REFERENCES

1. Zhu N, Zhang D, Wang W, Li X, Yang B, Song J, Zhao X, Huang B, Shi W, Lu R, Niu P, Zhan F, Ma X, Wang D, Xu W, Wu G, Gao GF, Tan W, China Novel Coronavirus Investigating and Research Team. 2020. A novel coronavirus from patients with pneumonia in China, 2019. N Engl J Med 382:727–733. https://doi.org/10.1056/NEJMoa2001017.
2. Huang C, Wang Y, Li X, Ren L, Zhao J, Hu Y, Zhang L, Fan G, Xu J, Gu X, Cheng Z, Yu T, Xia J, Wei Y, Wu W, Xie X, Yin W, Li H, Liu M, Xiao Y, Gao H, Guo L, Xie J, Wang G, Jiang R, Gao Z, Jin Q, Wang J, Cao B. 2020. Clinical features of patients infected with 2019 novel coronavirus in Wuhan, China. Lancet 395:497–506. https://doi.org/10.1016/S0140-6736(20)30183-5.
3. Mitsuya H, Kokudo N. 2020. Sustaining containment of COVID-19: global sharing for pandemic response. Glob Health Med 2:53–55. https://doi.org/10.35772/ghm.2020.01040.
4. Maciosek MV, LaFrance AB, Dehmer SP, McGree DA, Flottemesch TJ, Xu Z, Solberg LI. 2017. Updated priorities among effective clinical preventive services. Ann Fam Med 15:14–22. https://doi.org/10.1370/afm.2017.
5. Whitney CG, Zhou F, Singleton J, Schuchat A, Centers for Disease Control and Prevention (CDC). 2014. Benefits from immunization during the vaccines for children program era - United States, 1994–2013. MMWR Morb Mortal Wkly Rep 63:352–355.
6. Richman DD. 2021. COVID-19 vaccines: implementation, limitations and opportunities. Glob Health Med 3:1–5. https://doi.org/10.35772/ghm.2021.01010.
7. Walsh EE, Frenck RW, Jr, Falsey AR, Kitchin N, Absalon J, Gurtman A, Lockhart S, Neuzil K, Mulligan MJ, Bailey R, Swanson KA, Li P, Koury K, Kalina W, Cooper D, Fontes-Garfias C, Shi PY, Türeci Ö, Tompkins KR, Lyke KE, Raabe V, Dormitzer PR, Jansen KU, Şahin U, Gruber WC. 2020. Safety and immunogenicity of two RNA-based Covid-19 vaccine candidates. N Engl J Med 383:2439–2450. https://doi.org/10.1056/NEJMoa2027906.
8. Jackson LA, Anderson EJ, Rouphael NG, Roberts PC, Makhene M, Coler RN, McCullough MP, Chappell JD, Denison MR, Stevens LJ, Pruijssers AJ, McDermott A, Flach B, Doria-Rose NA, Corbett KS, Morabito KM, O'Dell S, Schmidt SD, Swanson PA, Padilla M, Mascola JR, Neuzil KM, Bennett H, Sun W, Peters E, Makowski M, Albert J, Cross K, Buchanan W, Pikaart-Tautges R, Ledgerwood JE, Graham BS, Beigel JH, mRNA-1273 Study Group. 2020. Beigel JHAn mRNA Vaccine against SARS-CoV-2 - preliminary report. N Engl J Med 383:1920–1931. https://doi.org/10.1056/NEJMoa2022483.
9. Folegatti PM, Ewer KJ, Aley PK, Angus B, Becker S, Belij-Rammerstorfer S, Bellamy D, Bibi S, Bittaye M, Clutterbuck EA, Dold C, Faust SN, Finn A, Flaxman AL, Hallis B, Heath P, Jenkin D, Lazarus R, Makinson R, Minassian AM, Pollock KM, Ramasamy M, Robinson H, Snape M, Tarrant R, Voysey M, Green C, Douglas AD, Hill AVS, Lambe T, Gilbert SC, Pollard AJ, Aboagye J, Adams K, Ali A, Allen E, Allison JL, Anslow R, Arbe-Barnes EH, Babbage G, Baillie K, Baker M, Baker N, Baker P, Baleanu I, Ballaminut J, Barnes E, Barrett J, Bates L, Batten A, et al. 2020. Safety and immunogenicity of the ChAdOx1 nCoV-19 vaccine against SARS-CoV-2: a preliminary report of a phase 1/2, single-blind, randomised controlled trial. Lancet 396:467–478. https://doi.org/10.1016/S0140-6736(20)31604-4.
10. Sadoff J, Le Gars M, Shukarev G, Heerwegh D, Truyers C, de Groot AM, Stoop J, Tete S, Van Damme W, Leroux-Roels I, Berghmans PJ, Kimmel M, Van Damme P, de Hoon J, Smith W, Stephenson KE, De Rosa SC, Cohen KW, McElrath MJ, Cormier E, Scheper G, Barouch DH, Hendriks J, Struyf F, Douoguih M, Van Hoof J, Schuitemaker H. 2021. Interim results of a phase 1-2a trial of Ad26.COV2.S Covid-19 vaccine. N Engl J Med 384:1824–1835. https://doi.org/10.1056/NEJMoa2034201.
11. Xia S, Duan K, Zhang Y, Zhao D, Zhang H, Xie Z, Li X, Peng C, Zhang Y, Zhang W, Yang Y, Chen W, Gao X, You W, Wang X, Wang Z, Shi Z, Wang Y, Yang X, Zhang L, Huang L, Wang Q, Lu J, Yang Y, Guo J, Zhou W, Wan X, Wu C, Wang W, Huang S, Du J, Meng Z, Pan A, Yuan Z, Shen S, Guo W, Yang X. 2020. Effect of an inactivated vaccine against SARS-CoV-2 on safety and immunogenicity outcomes: interim analysis of 2 randomized clinical trials. JAMA 324:951–960. https://doi.org/10.1001/jama.2020.15543.
12. Zhang Y, Zeng G, Pan H, Li C, Hu Y, Chu K, Han W, Chen Z, Tang R, Yin W, Chen X, Hu Y, Liu X, Jiang C, Li J, Yang M, Song Y, Wang X, Gao Q, Zhu F. 2021. Safety, tolerability, and immunogenicity of an inactivated SARS-CoV-2 vaccine in healthy adults aged 18–59 years: a randomised, double-blind, placebo-controlled, phase 1/2 clinical trial. Lancet Infect Dis 21:181–192. https://doi.org/10.1016/S1473-3099(20)30843-4.
13. Keech C, Albert G, Cho I, Robertson A, Reed P, Neal S, Plested JS, Zhu M, Cloney-Clark S, Zhou H, Smith G, Patel N, Frieman MB, Haupt RE, Logue J, McGrath M, Weston S, Piedra PA, Desai C, Callahan K, Lewis M, Price-Abbott P, Formica N, Shinde V, Fries L, Lickliter JD, Griffin P, Wilkinson B, Glenn GM. 2020. Phase 1–2 trial of a SARS-CoV-2 recombinant spike protein nanoparticle vaccine. N Engl J Med 383:2320–2332. https://doi.org/10.1056/NEJMoa2026920.
14. Ward BJ, Gobeil P, Séguin A, Atkins J, Boulay I, Charbonneau PY, Couture M, D'Aoust MA, Dhaliwall J, Finkle C, Hager K, Mahmood A, Makarkov A, Cheng MP, Pillet S, Schimke P, St-Martin S, Trépanier S, Landry N. 2021. Phase 1 randomized trial of a plant-derived virus-like particle vaccine for COVID-19. Nat Med 27:1071–1078. https://doi.org/10.1038/s41591-021-01370-1.
15. Dey A, Chozhavel Rajanathan TM, Chandra H, Pericherla HPR, Kumar S, Choonia HS, Bajpai M, Singh AK, Sinha A, Saini G, Dalal P, Vandriwala S, Raheem MA, Divate RD, Navlani NL, Sharma V, Parikh A, Prasath S, Sankar Rao M, Maithal K. 2021. Immunogenic potential of DNA vaccine candidate, ZyCoV-D against SARS-CoV-2 in animal models. Vaccine 39:4108–4116. https://doi.org/10.1016/j.vaccine.2021.05.098.
16. Richman DD. 2020. Antiviral drug discovery to address the COVID-19 pandemic. mBio 11:e02134-20. https://doi.org/10.1128/mBio.02134-20.
17. Davies NG, Abbott S, Barnard RC, Jarvis CI, Kucharski AJ, Munday JD, Pearson CAB, Russell TW, Tully DC, Washburne AD, Wenseleers T, Gimma A, Waites W, Wong KLM, van Zandvoort K, Silverman JD, Diaz-Ordaz K, Keogh R, Eggo RM, Funk S, Jit M, Atkins KE, Edmunds WJ. 2021. Estimated transmissibility and impact of SARS-CoV-2 lineage B.1.1.7 in England. Science 372:eabg3055. https://doi.org/10.1126/science.abg3055.
18. Xie X, Liu Y, Liu J, Zhang X, Zou J, Fontes-Garfias CR, Xia H, Swanson KA, Cutler M, Cooper D, Menachery VD, Weaver SC, Dormitzer PR, Shi PY. 2021. Neutralization of SARS-CoV-2 spike 69/70 deletion, E484K and N501Y variants by BNT162b2 vaccine-elicited sera. Nat Med 27:620–621. https://doi.org/10.1038/s41591-021-01270-4.
19. Beigel JH, Tomashek KM, Dodd LE, Mehta AK, Zingman BS, Kalil AC, Hohmann E, Chu HY, Luetkemeyer A, Kline S, Lopez de Castilla D, Finberg RW, Dierberg K, Tapson V, Hsieh L, Patterson TF, Paredes R, Sweeney DA, Short WR, Touloumi G, Lye DC, Ohmagari N, Oh MD, Ruiz-Palacios GM, Benfield T, Fätkenheuer G, Kortepeter MG, Atmar RL, Creech CB, Lundgren J, Babiker AG, Pett S, Neaton JD, Burgess TH, Bonnett T, Green M, Makowski M, Osinusi A, Nayak S, Lane HC, ACTT-1 Study Group Members. 2020. Remdesivir for the treatment of Covid-19 - final report. N Engl J Med 383:1813–1826. https://doi.org/10.1056/NEJMoa2007764.
20. Horby P, Lim WS, Emberson JR, Mafham M, Bell JL, Linsell L, Staplin N, Brightling C, Ustianowski A, Elmahi E, Prudon B, Green C, Felton T, Chadwick D, Rege K, Fegan C, Chappell LC, Faust SN, Jaki T, Jeffery K, Montgomery A, Rowan K, Juszczak E, Baillie JK, Haynes R, Landray MJ, RECOVERY Collaborative Group. 2021. Dexamethasone in hospitalized patients with Covid-19. N Engl J Med 384:693–704. https://doi.org/10.1056/NEJMoa2021436.
21. Kalil AC, Patterson TF, Mehta AK, Tomashek KM, Wolfe CR, Ghazaryan V, Marconi VC, Ruiz-Palacios GM, Hsieh L, Kline S, Tapson V, Iovine NM, Jain MK, Sweeney DA, El Sahly HM, Branche AR, Regalado Pineda J, Lye DC, Sandkovsky U, Luetkemeyer AF, Cohen SH, Finberg RW, Jackson PEH, Taiwo B, Paules CI, Arguinchona H, Erdmann N, Ahuja N, Frank M, Oh MD, Kim ES, Tan SY, Mularski RA, Nielsen H, Ponce PO, Taylor BS, Larson L, Rouphael NG, Saklawi Y, Cantos VD, Ko ER, Engemann JJ, Amin AN, Watanabe M, Billings J, Elie MC, Davey RT, Burgess TH, Ferreira J, Green M, et al. 2021. Baricitinib plus remdesivir for hospitalized adults with Covid-19. N Engl J Med 384:795–807. https://doi.org/10.1056/NEJMoa2031994.
22. Mehta P, McAuley DF, Brown M, Sanchez E, Tattersall RS, Manson JJ, HLH Across Speciality Collaboration, UK. 2020. COVID-19: consider cytokine storm syndromes and immunosuppression. Lancet 395:1033–1034. https://doi.org/10.1016/S0140-6736(20)30628-0.

23. Stone JH, Frigault MJ, Serling-Boyd NJ, Fernandes AD, Harvey L, Foulkes AS, Horick NK, Healy BC, Shah R, Bensaci AM, Woolley AE, Nikiforow S, Lin N, Sagar M, Schrager H, Huckins DS, Axelrod M, Pincus MD, Fleisher J, Sacks CA, Dougan M, North CM, Halvorsen YD, Thurber TK, Dagher Z, Scherer A, Wallwork RS, Kim AY, Schoenfeld S, Sen P, Neilan TG, Perugino CA, Unizony SH, Collier DS, Matza MA, Yinh JM, Bowman KA, Meyerowitz E, Zafar A, Drobni ZD, Bolster MB, Kohler M, D'Silva KM, Dau J, Lockwood MM, Cubbison C, Weber BN, Mansour MK, BACC Bay Tocilizumab Trial Investigators. 2020. Efficacy of tocilizumab in patients hospitalized with Covid-19. N Engl J Med 383:2333–2344. https://doi.org/10.1056/NEJMoa2028836.
24. Wang Y, Zhang D, Du G, Du R, Zhao J, Jin Y, Fu S, Gao L, Cheng Z, Lu Q, Hu Y, Luo G, Wang K, Lu Y, Li H, Wang S, Ruan S, Yang C, Mei C, Wang Y, Ding D, Wu F, Tang X, Ye X, Ye Y, Liu B, Yang J, Yin W, Wang A, Fan G, Zhou F, Liu Z, Gu X, Xu J, Shang L, Zhang Y, Cao L, Guo T, Wan Y, Qin H, Jiang Y, Jaki T, Hayden FG, Horby PW, Cao B, Wang C. 2020. Remdesivir in adults with severe COVID-19: a randomised, double-blind, placebo-controlled, multicentre trial. Lancet 395:1569–1578. https://doi.org/10.1016/S0140-6736(20)31022-9.
25. Chen P, Nirula A, Heller B, Gottlieb RL, Boscia J, Morris J, Huhn G, Cardona J, Mocherla B, Stosor V, Shawa I, Adams AC, Van Naarden J, Custer KL, Shen L, Durante M, Oakley G, Schade AE, Sabo J, Patel DR, Klekotka P, Skovronsky DM, BLAZE-1 Investigators. 2021. SARS-CoV-2 neutralizing antibody LY-CoV555 in outpatients with Covid-19. N Engl J Med 384:229–237. https://doi.org/10.1056/NEJMoa2029849.
26. Lundgren JD, Grund B, Barkauskas CE, Holland TL, Gottlieb RL, Sandkovsky U, Brown SM, Knowlton KU, Self WH, Files DC, Jain MK, Benfield T, Bowdish ME, Leshnower BG, Baker JV, Jensen JU, Gardner EM, Ginde AA, Harris ES, Johansen IS, Markowitz N, Matthay MA, Østergaard L, Chang CC, Davey VJ, Goodman A, Higgs ES, Murray DD, Murray TA, Paredes R, Parmar MKB, Phillips AN, Reilly C, Sharma S, Dewar RL, Teitelbaum M, Wentworth D, Cao H, Klekotka P, Babiker AG, Gelijns AC, Kan VL, Polizzotto MN, Thompson BT, Lane HC, Neaton JD, ACTIV-3/TICO LY-CoV555 Study Group. 2021. A neutralizing monoclonal antibody for hospitalized patients with Covid-19. N Engl J Med 384:905–914. https://doi.org/10.1056/NEJMoa2033130.
27. Horby PW, Mafham M, Peto L, Campbell M, Pessoa-Amorim G, Spata E, Staplin N, Emberson JR, Prudon B, Hine P, Brown T, Green CA, Sarkar R, Desai P, Yates B, Bewick T, Tiberi S, Felton T, Baillie JK, Buch MH, Chappell LC, Day JN, Faust SN, Jaki T, Jeffery K, Juszczak E, Lim WS, Montgomery A, Mumford A, Rowan K, Thwaites G, Weinreich DM, Haynes R, Landray MJ, RECOVERY Collaborative Group. 2021. Casirivimab and imdevimab in patients admitted to hospital with COVID-19 (RECOVERY): a randomised, controlled, open-label, platform trial. medRxiv https://doi.org/10.1101/2021.06.15.21258542.
28. Cathcart AL, Havenar-Daughton C, Lempp FA, Ma D, Schmid MA, Agostini ML, Guarino B, Di Iulio J, Rosen LE, Tucker H, Dillen J, Subramanian S, Sloan B, Bianchi S, Pinto D, Saliba C, Wojcechowskyj JA, Noack J, Zhou J, Kaiser H, Chase A, Montiel-Ruiz M, Dellota E, Jr, Park A, Spreafico R, Sahakyan A, Lauron EJ, Czudnochowski N, Cameroni E, Ledoux S, Werts A, Colas C, Soriaga L, Telenti A, Purcell LA, Hwang S, Snell G, Virgin HW, Corti D, Hebner CM. 2021. The dual function monoclonal antibodies VIR-7831 and VIR-7832 demonstrate potent in vitro and in vivo activity against SARS-CoV-2. bioRxiv https://doi.org/10.1101/2021.03.09.434607.
29. Siemieniuk RA, Bartoszko JJ, Ge L, Zeraatkar D, Izcovich A, Kum E, Pardo-Hernandez H, Qasim A, Martinez JPD, Rochwerg B, Lamontagne F, Han MA, Liu Q, Agarwal A, Agoritsas T, Chu DK, Couban R, Cusano E, Darzi A, Devji T, Fang B, Fang C, Flottorp SA, Foroutan F, Ghadimi M, Heels-Ansdell D, Honarmand K, Hou L, Hou X, Ibrahim Q, Khamis A, Lam B, Loeb M, Marcucci M, McLeod SL, Motaghi S, Murthy S, Mustafa RA, Neary JD, Rada G, Riaz IB, Sadeghirad B, Sekercioglu N, Sheng L, Sreekanta A, Switzer C, Tendal B, Thabane L, Tomlinson G, Turner T, et al. 2020. Drug treatments for covid-19: living systematic review and network meta-analysis. BMJ 370:m2980. https://doi.org/10.1136/bmj.m2980.
30. Hattori SI, Higashi-Kuwata N, Hayashi H, Allu SR, Raghavaiah J, Bulut H, Das D, Anson BJ, Lendy EK, Takamatsu Y, Takamune N, Kishimoto N, Murayama K, Hasegawa K, Li M, Davis DA, Kodama EN, Yarchoan R, Wlodawer A, Misumi S, Mesecar AD, Ghosh AK, Mitsuya H. 2021. A small molecule compound with an indole moiety inhibits the main protease of SARS-CoV-2 and blocks virus replication. Nat Commun 12:668. https://doi.org/10.1038/s41467-021-20900-6.
31. Zhang L, Lin D, Sun X, Curth U, Drosten C, Sauerhering L, Becker S, Rox K, Hilgenfeld R. 2020. Crystal structure of SARS-CoV-2 main protease provides a basis for design of improved α-ketoamide inhibitors. Science 368:409–412. https://doi.org/10.1126/science.abb3405.
32. Jin Z, Du X, Xu Y, Deng Y, Liu M, Zhao Y, Zhang B, Li X, Zhang L, Peng C, Duan Y, Yu J, Wang L, Yang K, Liu F, Jiang R, Yang X, You T, Liu X, Yang X, Bai F, Liu H, Liu X, Guddat LW, Xu W, Xiao G, Qin C, Shi Z, Jiang H, Rao Z, Yang H. 2020. Structure of M pro from SARS-CoV-2 and discovery of its inhibitors. Nature 582:289–293. https://doi.org/10.1038/s41586-020-2223-y.
33. Boras B, Jones RM, Anson BJ, Arenson D, Aschenbrenner L, Bakowski MA, Beutler N, Binder J, Chen E, Eng H, Hammond J, Hoffman R, Kadar EP, Kania R, Kimoto E, Kirkpatrick MG, Lanyon L, Lendy EK, Lillis JR, Luthra SA, Ma C, Noell S, Obach RS, O'Brien MN, O'Connor R, Ogilvie K, Owen D, Pettersson M, Reese MR, Rogers TF, Rossulek MI, Sathish JG, Steppan C, Ticehurst M, Updyke LW, Zhu Y, Wang J, Chatterjee AK, Mesecar AD, Anderson AS, Allerton C. 2020. Discovery of a novel inhibitor of coronavirus 3CL protease as a clinical candidate for the potential treatment of COVID-19. bioRxiv https://doi.org/10.1101/2020.09.12.293498.
34. Sheahan TP, Sims AC, Zhou S, Graham RL, Pruijssers AJ, Agostini ML, Leist SR, Schäfer A, Dinnon KH, III, Stevens LJ, Chappell JD, Lu X, Hughes TM, George AS, Hill CS, Montgomery SA, Brown AJ, Bluemling GR, Natchus MG, Saindane M, Kolykhalov AA, Painter G, Harcourt J, Tamin A, Thornburg NJ, Swanstrom R, Denison MR, Baric RS. 2020. An orally bioavailable broad-spectrum antiviral inhibits SARS-CoV-2 in human airway epithelial cell cultures and multiple coronaviruses in mice. Sci Transl Med 12:eabb5883. https://doi.org/10.1126/scitranslmed.abb5883.
35. Carter PJ, Lazar GA. 2018. Next generation antibody drugs: pursuit of the 'high-hanging fruit.' Nat Rev Drug Discov 17:197–223. https://doi.org/10.1038/nrd.2017.227.
36. Piechotta V, Iannizzi C, Chai KL, Valk SJ, Kimber C, Dorando E, Monsef I, Wood EM, Lamikanra AA, Roberts DJ, McQuilten Z, So-Osman C, Estcourt LJ, Skoetz N. 2021. Convalescent plasma or hyperimmune immunoglobulin for people with COVID-19: a living systematic review. Cochrane Database Syst Rev 5:CD013600. https://doi.org/10.1002/14651858.CD013600.pub4.
37. Salazar E, Christensen PA, Graviss EA, Nguyen DT, Castillo B, Chen J, Lopez BV, Eagar TN, Yi X, Zhao P, Rogers J, Shehabeldin A, Joseph D, Masud F, Leveque C, Olsen RJ, Bernard DW, Gollihar J, Musser JM. 2021. Significantly decreased mortality in a large cohort of coronavirus disease 2019 (COVID-19) patients transfused early with convalescent plasma containing high-titer anti–severe acute respiratory syndrome coronavirus 2 (SARS-CoV-2) spike protein IgG. Am J Pathol 191:90–107. https://doi.org/10.1016/j.ajpath.2020.10.008.
38. Libster R, Pérez Marc G, Wappner D, Coviello S, Bianchi A, Braem V, Esteban I, Caballero MT, Wood C, Berrueta M, Rondan A, Lescano G, Cruz P, Ritou Y, Fernández Viña V, Álvarez Paggi D, Esperante S, Ferreti A, Ofman G, Ciganda Á, Rodriguez R, Lantos J, Valentini R, Itcovici N, Hintze A, Oyarvide ML, Etchegaray C, Neira A, Name I, Alfonso J, López Castelo R, Caruso G, Rapelius S, Alvez F, Etchenique F, Dimase F, Alvarez D, Aranda SS, Sánchez Yanotti C, De Luca J, Jares Baglivo S, Laudanno S, Nowogrodzki F, Larrea R, Silveyra M, Leberzstein G, Debonis A, Molinos J, González M, Perez E, et al. 2021. Early high-titer plasma therapy to prevent severe Covid-19 in older adults. N Engl J Med 384:610–618. https://doi.org/10.1056/NEJMoa2033700.
39. Imai M, Iwatsuki-Horimoto K, Hatta M, Loeber S, Halfmann PJ, Nakajima N, Watanabe T, Ujie M, Takahashi K, Ito M, Yamada S, Fan S, Chiba S, Kuroda M, Guan L, Takada K, Armbrust T, Balogh A, Furusawa Y, Okuda M, Ueki H, Yasuhara A, Sakai-Tagawa Y, Lopes TJS, Kiso M, Yamayoshi S, Kinoshita N, Ohmagari N, Hattori SI, Takeda M, Mitsuya H, Krammer F, Suzuki T, Kawaoka Y. 2020. Syrian hamsters as a small animal model for SARS-CoV-2 infection and countermeasure development. Proc Natl Acad Sci U S A 117:16587–16595. https://doi.org/10.1073/pnas.2009799117.
40. Maeda K, Higashi-Kuwata N, Kinoshita N, Kutsuna S, Tsuchiya K, Hattori S-I, Matsuda K, Takamatsu Y, Gatanaga H, Oka S, Sugiyama H, Ohmagari N, Mitsuya H. 2021. Neutralization of SARS-CoV-2 with IgG from COVID-19 convalescent plasma. Sci Rep 11:5563. https://doi.org/10.1038/s41598-021-84733-5.
41. Zhou D, Chan JF, Zhou B, Zhou R, Li S, Shan S, Liu L, Zhang AJ, Chen SJ, Chan CC, Xu H, Poon VK, Yuan S, Li C, Chik KK, Chan CC, Cao J, Chan CY, Kwan KY, Du Z, Lau TT, Zhang Q, Zhou J, To KK, Zhang L, Ho DD, Yuen KY, Chen Z. 2021. Robust SARS-CoV-2 infection in nasal turbinates after treatment with systemic neutralizing antibodies. Cell Host Microbe 29:551–563.e5. https://doi.org/10.1016/j.chom.2021.02.019.
42. Haagmans BL, Noack D, Okba NMA, Li W, Wang C, Bestebroer T, de Vries R, Herfst S, de Meulder D, Verveer E, van Run P, Lamers MM, Rijnders B, Rokx C, van Kuppeveld F, Grosveld F, Drabek D, Geurts van Kessel C, Koopmans M, Bosch BJ, Kuiken T, Rockx B. 2021. SARS-CoV-2 neutralizing human antibodies protect against lower respiratory tract disease in a hamster model. J Infect Dis 223:2020–2028. https://doi.org/10.1093/infdis/jiab289.

43. Chan JF, Zhang AJ, Yuan S, Poon VK, Chan CC, Lee AC, Chan WM, Fan Z, Tsoi HW, Wen L, Liang R, Cao J, Chen Y, Tang K, Luo C, Cai JP, Kok KH, Chu H, Chan KH, Sridhar S, Chen Z, Chen H, To KK, Yuen KY. 2020. Simulation of the clinical and pathological manifestations of coronavirus disease 2019 (COVID-19) in a golden Syrian hamster model: implications for disease pathogenesis and transmissibility. Clin Infect Dis 71:2428–2446. https://doi.org/10.1093/cid/ciaa325.
44. Luke TC, Kilbane EM, Jackson JL, Hoffman SL. 2006. Meta-analysis: convalescent blood products for Spanish influenza pneumonia: a future H5N1 treatment? Ann Intern Med 145:599–609. https://doi.org/10.7326/0003-4819-145-8-200610170-00139.
45. Klassen SA, Senefeld JW, Johnson PW, Carter RE, Wiggins CC, Shoham S, Grossman BJ, Henderson JP, Musser J, Salazar E, Hartman WR, Bouvier NM, Liu STH, Pirofski LA, Baker SE, van Helmond N, Wright RS, Fairweather D, Bruno KA, Wang Z, Paneth NS, Casadevall A, Joyner MJ. 2021. The effect of convalescent plasma therapy on mortality among patients with COVID-19: systematic review and meta-analysis. Mayo Clin Proc 96:1262–1275. https://doi.org/10.1016/j.mayocp.2021.02.008.
46. Alfi O, Yakirevitch A, Wald O, Wandel O, Izhar U, Oiknine-Djian E, Nevo Y, Elgavish S, Dagan E, Madgar O, Feinmesser G, Pikarsky E, Bronstein M, Vorontsov O, Jonas W, Ives J, Walter J, Zakay-Rones Z, Oberbaum M, Panet A, Wolf DG. 2021. Human nasal and lung tissues infected ex vivo with SARS-CoV-2 provide insights into differential tissue-specific and virus-specific innate immune responses in the upper and lower respiratory tract. J Virol 95:e0013021. https://doi.org/10.1128/JVI.00130-21.
47. Grifoni A, Weiskopf D, Ramirez SI, Mateus J, Dan JM, Moderbacher CR, Rawlings SA, Sutherland A, Premkumar L, Jadi RS, Marrama D, de Silva AM, Frazier A, Carlin AF, Greenbaum JA, Peters B, Krammer F, Smith DM, Crotty S, Sette A. 2020. Targets of T cell responses to SARS-CoV-2 coronavirus in humans with COVID-19 disease and unexposed individuals. Cell 181:1489–1501. https://doi.org/10.1007/s10875-021-01046-y.
48. Dan JM, Mateus J, Kato Y, Hastie KM, Yu ED, Faliti CE, Grifoni A, Ramirez SI, Haupt S, Frazier A, Nakao C, Rayaprolu V, Rawlings SA, Peters B, Krammer F, Simon V, Saphire EO, Smith DM, Weiskopf D, Sette A, Crotty S. 2021. Immunological memory to SARS-CoV-2 assessed for up to 8 months after infection. Science 371:eabf4063. https://doi.org/10.1126/science.abf4063.
49. Kristiansen PA, Page M, Bernasconi V, Mattiuzzo G, Dull P, Makar K, Plotkin S, Knezevic I. 2021. WHO International Standard for anti-SARS-CoV-2 immunoglobulin. Lancet 397:1347–1348. https://doi.org/10.1016/S0140-6736(21)00527-4.
50. Noy-Porat T, Makdasi E, Alcalay R, Mechaly A, Levy Y, Bercovich-Kinori A, Zauberman A, Tamir H, Yahalom-Ronen Y, Israeli M, Epstein E, Achdout H, Melamed S, Chitlaru T, Weiss S, Peretz E, Rosen O, Paran N, Yitzhaki S, Shapira SC, Israely T, Mazor O, Rosenfeld R. 2020. A panel of human neutralizing mAbs targeting SARS-CoV-2 spike at multiple epitopes. Nat Commun 11:4303. https://doi.org/10.1038/s41467-020-18159-4.
51. Rodda LB, Netland J, Shehata L, Pruner KB, Morawski PA, Thouvenel CD, Takehara KK, Eggenberger J, Hemann EA, Waterman HR, Fahning ML, Chen Y, Hale M, Rathe J, Stokes C, Wrenn S, Fiala B, Carter L, Hamerman JA, King NP, Gale M, Jr, Campbell DJ, Rawlings DJ, Pepper M. 2021. Functional SARS-CoV-2-specific immune memory persists after mild COVID-19. Cell 184:169–183. https://doi.org/10.1016/j.cell.2020.11.029.
52. Baric RS. 2020. Emergence of a highly fit SARS-CoV-2 variant. N Engl J Med 383:2684–2686. https://doi.org/10.1056/NEJMcibr2032888.
53. Frampton D, Rampling T, Cross A, Bailey H, Heaney J, Byott M, Scott R, Sconza R, Price J, Margaritis M, Bergstrom M, Spyer MJ, Miralhes PB, Grant P, Kirk S, Valerio C, Mangera Z, Prabhahar T, Moreno-Cuesta J, Arulkumaran N, Singer M, Shin GY, Sanchez E, Paraskevopoulou SM, Pillay D, McKendry RA, Mirfenderesky M, Houlihan CF, Nastouli E. 2021. Genomic characteristics and clinical effect of the emergent SARS-CoV-2 B.1.1.7 lineage in London, UK: a whole-genome sequencing and hospital-based cohort study. Lancet Infect Dis 21:1246–1256. https://doi.org/10.1016/S1473-3099(21)00170-5.
54. Tegally H, Wilkinson E, Giovanetti M, Iranzadeh A, Fonseca V, Giandhari J, Doolabh D, Pillay S, San EJ, Msomi N, Mlisana K, von Gottberg A, Walaza S, Allam M, Ismail A, Mohale T, Glass AJ, Engelbrecht S, Van Zyl G, Preiser W, Petruccione F, Sigal A, Hardie D, Marais G, Hsiao NY, Korsman S, Davies MA, Tyers L, Mudau I, York D, Maslo C, Goedhals D, Abrahams S, Laguda-Akingba O, Alisoltani-Dehkordi A, Godzik A, Wibmer CK, Sewell BT, Lourenço J, Alcantara LCJ, Kosakovsky Pond SL, Weaver S, Martin D, Lessells RJ, Bhiman JN, Williamson C, de Oliveira T. 2021. Detection of a SARS-CoV-2 variant of concern in South Africa. Nature 592:438–443. https://doi.org/10.1038/s41586-021-03402-9.
55. Faria NR, Mellan TA, Whittaker C, Claro IM, Candido DDS, Mishra S, Crispim MAE, Sales FCS, Hawryluk I, McCrone JT, Hulswit RJG, Franco LAM, Ramundo MS, de Jesus JG, Andrade PS, Coletti TM, Ferreira GM, Silva CAM, Manuli ER, Pereira RHM, Peixoto PS, Kraemer MUG, Gaburo N, Jr, Camilo CDC, Hoeltgebaum H, Souza WM, Rocha EC, de Souza LM, de Pinho MC, Araujo LJT, Malta FSV, de Lima AB, Silva JDP, Zauli DAG, Ferreira ACS, Schnekenberg RP, Laydon DJ, Walker PGT, Schlüter HM, Dos Santos ALP, Vidal MS, Del Caro VS, Filho RMF, Dos Santos HM, Aguiar RS, Proença-Modena JL, Nelson B, Hay JA, Monod M, Miscouridou X, et al. 2021. Genomics and epidemiology of the P.1 SARS-CoV-2 lineage in Manaus. Science 372:815–821. https://doi.org/10.1126/science.abh2644.
56. Shen X, Tang H, Pajon R, Smith G, Glenn GM, Shi W, Korber B, Montefiori DC. 2021. Neutralization of SARS-CoV-2 Variants B.1.429 and B.1.351. N Engl J Med 384:2352–2354. https://doi.org/10.1056/NEJMc2103740.
57. Zhou B, Thao TTN, Hoffmann D, Taddeo A, Ebert N, Labroussaa F, Pohlmann A, King J, Steiner S, Kelly JN, Portmann J, Halwe NJ, Ulrich L, Trüeb BS, Fan X, Hoffmann B, Wang L, Thomann L, Lin X, Stalder H, Pozzi B, de Brot S, Jiang N, Cui D, Hossain J, Wilson MM, Keller MW, Stark TJ, Barnes JR, Dijkman R, Jores J, Benarafa C, Wentworth DE, Thiel V, Beer M. 2021. SARS-CoV-2 spike D614G change enhances replication and transmission. Nature 592:122–127. https://doi.org/10.1038/s41586-021-03361-1.
58. Sekizuka T, Itokawa K, Hashino M, Kawano-Sugaya T, Tanaka R, Yatsu K, Ohnishi A, Goto K, Tsukagoshi H, Ehara H, Sadamasu K, Taira M, Shibata S, Nomoto R, Hiroi S, Toho M, Shimada T, Matsui T, Sunagawa T, Kamiya H, Yahata Y, Yamagishi T, Suzuki M, Wakita T, Kuroda MA. 2020. Genome epidemiological study of SARS-CoV-2 introduction into Japan. mSphere 5:e00786-20. https://doi.org/10.1128/mSphere.00786-20.
59. Hattori S-i, Higshi-Kuwata N, Raghavaiah J, Das D, Bulut H, Davis DA, Takamatsu Y, Matsuda K, Takamune N, Kishimoto N, Okamura T, Misumi S, Yarchoan R, Maeda K, Ghosh AK, Mitsuya H. 2020. GRL-0920, an indole chloropyridinyl ester, completely blocks SARS-CoV-2 infection. mBio 11:e01833-20. https://doi.org/10.1128/mBio.01833-20.
60. Draper NR, Smith H. 1966. Applied regression analysis. John Wiley & Sons, New York, NY.